Journal of Computer-Aided Molecular Design (2006) 20: 13–25
DOI 10.1007/s10822-005-9032-0

Force-field parametrization of retro-inverso modified residues: Development of torsional and electrostatic parameters

David Curcó[a], Francisco Rodríguez-Ropero[b] & Carlos Alemán[b,*]
[a]*Departament d'Enginyeria Química, Facultat de Química, Universitat de Barcelona, Martí i Franquès 1, E-08028, Barcelona, Spain;* [b]*Departament d'Enginyeria Química, E.T.S. d'Enginyers Industrials de Barcelona, Universitat Politécnica de Catalunya, Diagonal 647, E-08028, Barcelona, Spain*

Received 15 September 2005; accepted in revised form 17 November 2005

Key words: amino acid, force-field, parametrization, torsional energy, retro-inverso modification, amino acid

Summary

Torsional and the electrostatic parameters for molecular mechanics studies of retro-inverso modified peptides have been developed using quantum mechanical calculations. The resulting parameters have been compared with those calculated for conventional peptides. Rotational profiles, which were obtained spanning the corresponding dihedral angle, were corrected by removing the energy contributions associated to changes in interactions different from torsion under study. For this purpose, the torsional energy associated to each point of the profiles was estimated as the corresponding quantum mechanical energy minus the bonding and nonbonding energy contributions produced by the perturbations that the variation of the spanned dihedral angle causes in the bond distances, bond angles and the other dihedral angles. These energies were calculated using force-field expressions. The corrected profiles were fitted to a three-term Fourier expansion to derive the torsional parameters. Atomic charges for retro-inverso modified residues were derived from the rigorously calculated quantum mechanical electrostatic potential. Furthermore, the reliability of electrostatic models based on geometry-dependent charges and fixed charges has been examined.

Introduction

Computational methods based on Molecular Mechanics (MM), *i.e.* Molecular Dynamics (MD) and Monte Carlo (MC), are currently used in a large number of studies of (bio)molecular systems. Such techniques provide valuable information in various fields such as the structure and dynamics of small and large molecules, the interaction of between (macro)molecules, the study of solvation and other environmental effects, the formation of macromolecular assemblies, the diffusion of small molecules through pores and membranes, etc.

In MM the molecular energy consists of bonded (stretching, bending and torsion) and nonbonded terms (van der Waals and electrostatic):

$$E^{\mathrm{MM}} = E_{\mathrm{stretching}} + E_{\mathrm{bending}} + E_{\mathrm{torsion}} + E_{\mathrm{vdW}} + E_{\mathrm{electrostatic}} \quad (1)$$

All these terms are represented using very simple equations (the force-field), where different parameters guarantee the ability of the method to reproduce the properties of the system. This

*To whom correspondence should be addressed. E-mail: carlos.aleman@upc.es

explains the large research effort focused on both the improvement of the equations to evaluate these terms and the parameters appearing in such equations, which have been reflected in the development of several force-field [1–8]. Force-field parametrization can be performed using information derived from either experiments or quantum mechanical (QM) calculations. Experimentally based strategies are *a priori* the best choice, since it guarantees the fitting with experimental data [1, 3, 7–10]. However, such a parametrization is often impossible due to the lack of suitable experimental information, and consequently QM methods are applied to determine force-field parameters.

On the other hand, the study of bioactive peptide analogues, where some naturally occurring amino acids are substituted by modified amino acids, is a subject of considerable interest. Thus, modified amino acids are usually employed as building blocks in molecular engineering since they can be used to control the peptide secondary structure [11, 12], and to design molecules with enhanced resistance to biodegradation but retaining the biological response of bioactive peptides [13, 14]. Modifications may involve changes in the amino acid side chain or alteration of the amide bond. A potential advantage of the latter is that introduction of modified peptide links makes it possible to influence the biological properties of a molecule but retaining the receptor binding ability, which usually depends of the side chains [15].

The retro-inverso modification in a peptide chain, *i.e.* reversal of the direction of the amide bond, has been successfully incorporated to many bioactive peptides [16–25]. Furthermore, the retro-inverso amide bonds are also relevant in polymer science, since several families of well-studied synthetic polyamides involve a retro-inverso glycine residue as a part of their chemical repeating unit [26–28]. The conformational impact of retro-inverso modification on different amino acids, *i.e.* glycine, alanine, valine and dehydroalanine, has been investigated by our group using ab initio QM methods [29–33]. QM calculations were also used in molecular engineering applications devoted to stabilize a given structural motif using retro-modified peptides based on α-aminoisobutyric [11] and glycine [34, 35]. Conformational analysis of retro-inverso modified amino acids has been also performed using simulations based on MM [36–38]. Unfortunately, in some cases the results provided by these calculations were not in agreement with those obtained using QM suggesting that the parameters used in the force-field were not suitable to represent the properties of these compounds.

The increasing apparition of studies devoted to design new classes of peptidomimetics with biological activity using retro-inverso modifications of the amide bond indicates a renewed interest in this field [16–25]. Therefore, the development of reliable force-field parameters to perform MM simulations of these biomolecules is highly desirable. In this work, we use QM calculations to investigate the torsional and electrostatic parameters of malonamide, 2-methyl-malonamide, diaminomethane and diaminoethane residues, which correspond to all the possible retro-inverso modifications of a glycine and alanine units. More specifically, calculations were performed on *N*,*N*′-dimethylmalonamide (**1**), *N*,*N*′-dimethyl-2-methylmalonamide (**2**), bis(acetamide)methane (**3**) and 1,1-bis(acetamide)ethane (**4**). Additionally, a parallel study on *N*-acetylglycine-*N*′-methylamide (**5**) and *N*-acetylalanine-*N*′-methylamide (**6**), *i.e.* glycine and alanine dipeptides, was carried out for the sake of comparison. The six molecules investigated in this work are depicted in Figure 1.

Methods and computational details

Calculations were performed at the HF and B3LYP levels combined with the $6{-}31+G(d,\ p)$ basis set. Rotational profiles were computed spanning the corresponding dihedral angle, defined as indicates in Figure 1, in steps of 30°. In order to avoid undesirable conformational transitions, the contiguous flexible dihedral angle was frozen at 180°. A flexible rotor approximation was used in all cases. Thus, the structure in each point of the profile was obtained from geometry optimization at fixed dihedrals values.

On the other hand, MM energies have been computed using the analytical potential function of the Amber force-field, which is commonly used to study the dynamics of peptides and proteins [1]. In detail it presents the following functional form:

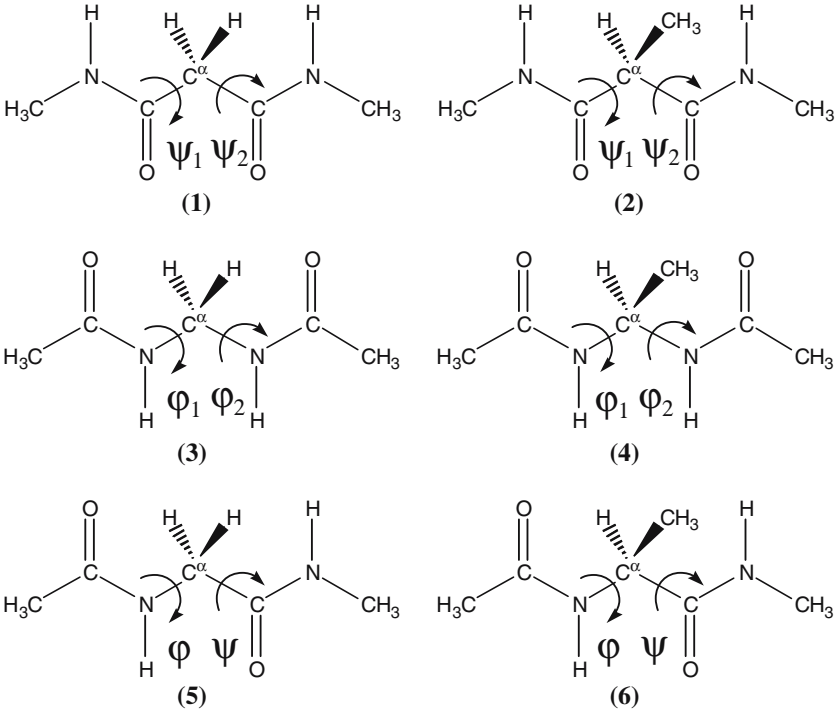

Figure 1. Compounds investigated in this work.

$$
\begin{aligned}
E^{\mathrm{MM}} = & \sum_{\text{bonds}} k_{\mathrm{str}}(r_{ij} - r_{ij}^{\mathrm{eq}})^2 \\
& + \sum_{\text{angles}} k_{\mathrm{bnd}}(\theta_{ij} - \theta_{ij}^{\mathrm{eq}})^2 \\
& + \sum_{\text{dihedrals}} \frac{V_n}{2}[1 + \cos(n\varphi - \gamma_n)] \\
& + \sum_{\text{nonbonded pairs}} \left[\frac{A_{ij}}{r_{ij}^{12}} - \frac{B_{ij}}{r_{ij}^{6}}\right] \\
& + \sum_{\text{nonbonded pairs}} \frac{q_i q_j}{\varepsilon r_{ij}}
\end{aligned}
\tag{2}
$$

In this equation, the first term represents the covalent bond stretching, the second describes the bond angle bending, while the third are the dihedral interactions. The last two terms of the molecular mechanics energy describe the nonbonding interactions: van der Waals and electrostatics.

The parametrization procedure used in this work is based on the PAPQMD strategy (Program for Approximate Parametrization from Quantum Mechanical Data) developed by Alemán and Orozco [39]. In this procedure, the quantum mechanical energies derived from the rotational profile analysis (ΔE^{QM}) are used in Equation 3, which provide the parameters by minimizing the squared difference between the MM and QM energies.

$$
\left(\Delta E^{\mathrm{QM}} - \Delta E^{\mathrm{MM}}\right)^2 = \text{minimum} \tag{3}
$$

ΔE^{MM} is expressed (Equation 4) as the sum of the energy related to the variation of the dihedral angle j ($\Delta E_{\mathrm{torsion}}(j)$) and the energy related to all the other variations in the molecular geometry (ΔE^{per}).

$$
\Delta E^{\mathrm{MM}} = \Delta E_{\mathrm{torsion}}(j) + \Delta E^{\mathrm{per}} \tag{4}
$$

Considering Equation 4, Equation 3 can be rewritten as:

$$
\left(\Delta E^{\mathrm{QM}} - \Delta E_{\mathrm{torsion}}(j) - \Delta E^{\mathrm{per}}\right)^2 = \text{minimum} \tag{5}
$$

As can be deduced from Equation 1, if the variation in the molecular geometry involves both bonding and nonbonding interactions, ΔE^{per} is expressed as:

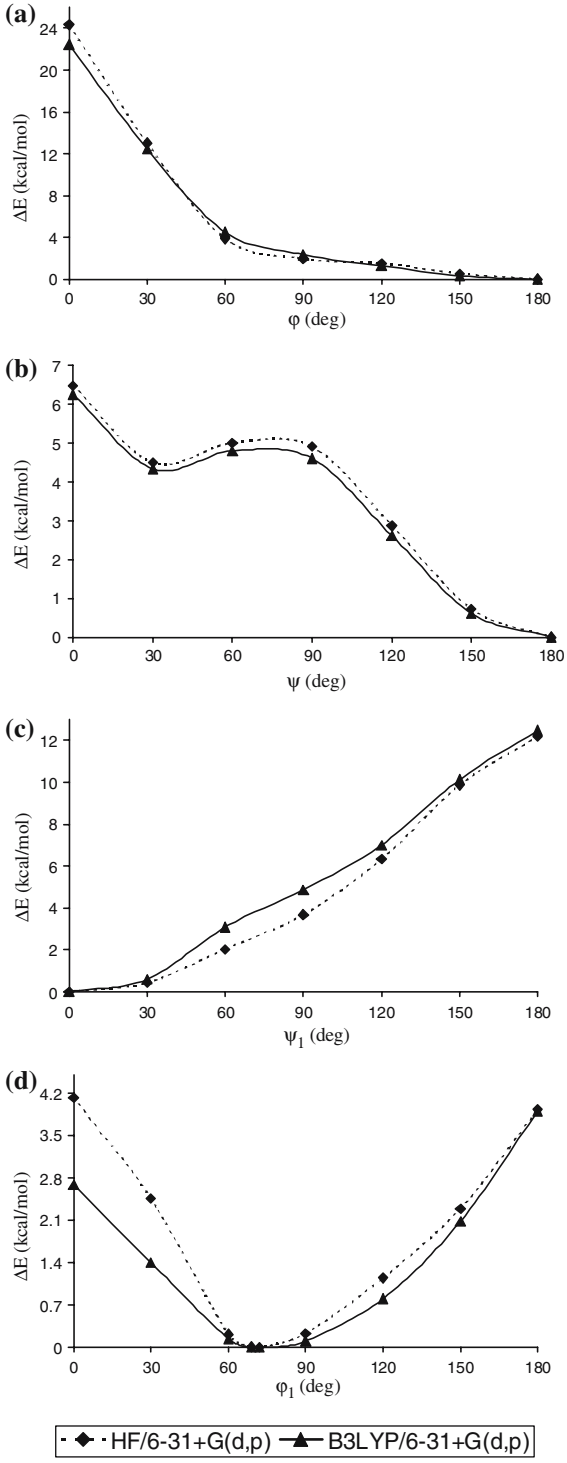

Figure 2. Quantum mechanical energy (ΔE^{QM}) profiles of the (a) N–C^{α} and (b) C^{α}–C rotations of **5** [$E(\varphi, \psi = 180°)$ and $E = E(\varphi = 180°, \psi)$, respectively], (c) the C–C^{α} rotation of **1** [$E = E(\psi_1, \psi_2 = 180°)$], and (d) the N–$C^{\alpha}$ rotation of **3** [$E = E(\varphi_1, \varphi_2 = 180°)$]. All the profiles were calculated at the HF/6−31 + *G*(*d*, *p*) and B3LYP/6−31 + *G*(*d*, *p*) levels.

$$\Delta E^{per} = \Delta E_{stretching} + \Delta E_{bending} + \Delta E_{torsion}(i \neq j) + \Delta E_{vdW} + \Delta E_{electrostatic} \quad (6)$$

where $\Delta E_{torsion}$ ($i \neq j$) refers to the variation of all the dihedral angles different from *j*. All the MM energy terms were computed according to the potential described in Equation 2.

The PAPQMD procedure has been successfully used for the parametrization of stretching and bending force constants (k_{str} and k_{bnd}, respectively, in Equation 2) of DNA bases [40], modified amino acids [31, 41], drugs [42], polymers [43], and natural products [44] as well as to develop torsional parameters for some simple organic molecules [43, 44]. However, the influence of the bonding and nonbonding interactions in the torsional profiles used in the parametrization procedure (Equations 5 and 6) has not been examined previously. In the present work, the contribution produced by such interactions in the torsional parameters will be analyzed in detail. Furthermore, we will investigate how the strategy used to describe the electrostatic interactions affects to the parametrization of the torsional term. More specifically, fixed and conformationally dependent charges will be considered in Equation 6 for the evaluation of the electrostatic energy.

Atomic charges were derived in all cases by fitting the HF/6−31 + *G*(*d*, *p*) quantum mechanical and the Coulombic molecular electrostatic potentials (MEPs) in a large set of points placed outside the nuclear region. The quality of the electrostatic parameters provided by this parametrization procedure is fully compatible with current force-fields.

Results and discussion

Parametrization of glycine and its retro-inverso modified analogues

Rotational profiles derived from quantum mechanical calculations

The rotational profiles $E = E(\varphi, \psi = 180°)$ and $E = E(\varphi = 180°, \psi)$ were calculated for the glycine dipeptide **5** at the HF/6−31 + *G*(*d*, *p*) and B3LYP/6−31 + *G*(*d*, *p*) levels. Figure 2a and b show the variation ΔE^{QM} vs. φ and ψ, respectively. The higher energy conformations are due to the

C=O···O=C and N–H···H–N repulsive interactions, which are maximum at φ, $\psi = (0°,180°)$ and φ, $\psi = (180°,0°)$, respectively. The energy difference between such two conformations indicates that the former interaction is about 16–18 kcal/mol more unfavorable than the latter. Furthermore, the two profiles show a minimum at φ, $\psi = (180°,180°)$, which corresponds to the C_5 conformation of the glycine dipeptide [45, 46].

The profiles $E = E(\psi_1,\psi_2 = 180°)$ and $E = E(\varphi_1,\varphi_2 = 180°)$ calculated for **1** and **3** are displayed in Figure 2c and d, respectively. As can be seen, retro-inverso modification on glycine dipeptide induces drastic changes in the conformational profiles. For **1**, the position of minimum energy is located at $\psi_1,\psi_2 = (0°, 180°)$ since the strong repulsive interactions between the two carbonyl groups are minimized. Furthermore, the highest energy conformation, which appears at ψ_1, $\psi_2 = (180°, 180°)$, is about 12 kcal/mol less unfavored than that found for **5** at φ, $\psi = (0°, 180°)$. Thus, although the C=O···O=C repulsive interactions are maximum in such two conformations, the changes produced by retro-inverso modification in the electronic structure of **1** alters the strength of such interaction. For **3** the minimum energy arrangement appears at φ_1, $\varphi_2 = (\sim 70°, 180°)$ indicating also a substantial change in the electronic structure with respect to **5**. Furthermore, the energy of the least favored arrangement is about 2 kcal/mol less unfavored for the former compound than for the latter one.

It should be emphasized that in all four cases HF/6–31 + *G*(*d*, *p*) and B3LYP/6–31 + *G*(*d*, *p*) calculations led to very similar results. Thus, electron correlation effects are expected to be very important in processes that involve formation or rupture of chemical bonds, but not in the conformational

Table 1. Fitted parameters for the torsional potentials of glycine dipeptide and its retro-inverso modified analogues.

Level	ΔE^{per}	**5** (N–C^{α})		**5** (C^{α}–C)		**1**		**3**	
		Parameters	r^2	Parameters	r^2	Parameters	r^2	Parameters	r^2
HF	0		0.97		0.95		1.00		0.96
		$V_1 = 16.0$ ($\gamma = 0°$),		$V_1 = 5.0$ ($\gamma = 0°$),		$V_1 = 10.8$ ($\gamma = 180°$),		$V_1 = 0.2$ ($\gamma = 180°$),	
		$V_2 = -10.8$ ($\gamma = 180°$),		$V_2 = 1.5$ ($\gamma = 180°$),		$V_2 = -2.4$ ($\gamma = 180°$),		$V_2 = 3.9$ ($\gamma = 0°$),	
		$V_3 = 6.4$ ($\gamma = 0°$)		$V_3 = 0.7$ ($\gamma = 0°$)		$V_3 = 1.1$ ($\gamma = 180°$)		$V_3 = -0.6$ ($\gamma = 0°$)	
B3LYP	0		0.95		0.94		1.00		0.93
		$V_1 = 15.5$ ($\gamma = 0°$),		$V_1 = 4.9$ ($\gamma = 0°$),		$V_1 = 10.8$ ($\gamma = 180°$),		$V_1 = -0.9$ ($\gamma = 0°$),	
		$V_2 = -9.5$ ($\gamma = 180°$),		$V_2 = 1.4$ ($\gamma = 180°$),		$V_2 = -1.3$ ($\gamma = 180°$),		$V_2 = 3.4$ ($\gamma = 0°$),	
		$V_3 = 5.3$ ($\gamma = 0°$)		$V_3 = 0.6$ ($\gamma = 0°$)		$V_3 = 1.4$ ($\gamma = 180°$)		$V_3 = 0.1$ ($\gamma = 0°$)	
HF	$\Delta E_{bonding}$		0.95		1.00		0.95		0.83
		$V_1 = -7.0$ ($\gamma = 180°$),		$V_1 = 0.1$ ($\gamma = 0°$),		$V_1 = 10.0$ ($\gamma = 180°$),		$V_1 = 0.9$ ($\gamma = 0°$),	
		$V_2 = 7.0$ ($\gamma = 0°$),		$V_2 = 3.5$ ($\gamma = 180°$),		$V_2 = -4.3$ ($\gamma = 180°$),		$V_2 = 1.4$ ($\gamma = 0°$),	
		$V_3 = 4.6$ ($\gamma = 0°$)		$V_3 = 2.0$ ($\gamma = 180°$)		$V_3 = 1.7$ ($\gamma = 0°$)		$V_3 = 2.3$ ($\gamma = 0°$)	
B3LYP	$\Delta E_{bonding}$		0.94		1.00		0.96		0.88
		$V_1 = -6.3$ ($\gamma = 180°$),		$V_1 = 0.0$ ($\gamma = 0°$),		$V_1 = 10.2$ ($\gamma = 180°$),		$V_1 = 0.2$ ($\gamma = 0°$),	
		$V_2 = 7.3$ ($\gamma = 0°$),		$V_2 = 3.8$ ($\gamma = 180°$),		$V_2 = -3.0$ ($\gamma = 180°$),		$V_2 = 1.6$ ($\gamma = 0°$),	
		$V_3 = 3.8$ ($\gamma = 0°$)		$V_3 = 2.1$ ($\gamma = 180°$)		$V_3 = 0.8$ ($\gamma = 0°$)		$V_3 = 2.3$ ($\gamma = 0°$)	
HF	$\Delta E_{bonding}-$		0.98		0.99		0.95		0.90
	$\Delta E_{nonbonding}$	$V_1 = 4.7$ ($\gamma = 0°$),		$V_1 = 2.2$ ($\gamma = 180°$),		$V_1 = 5.8$ ($\gamma = 0°$),		$V_1 = 2.0$ ($\gamma = 180°$),	
		$V_2 = -2.0$ ($\gamma = 180°$),		$V_2 = 4.2$ ($\gamma = 180°$),		$V_2 = -3.7$ ($\gamma = 180°$),		$V_2 = 2.3$ ($\gamma = 0°$)	
		$V_3 = 0.4$ ($\gamma = 0°$)		$V_3 = 2.4$ ($\gamma = 180°$)		$V_3 = 1.4$ ($\gamma = 0°$)		$V_3 = 2.0$ ($\gamma = 0°$)	
B3LYP	$\Delta E_{bonding}-$		0.94		0.99		0.90		0.85
	$\Delta E_{nonbonding}$	$V_1 = 4.2$ ($\gamma = 0°$),		$V_1 = 2.7$ ($\gamma = 180°$),		$V_1 = 4.4$ ($\gamma = 0°$),		$V_1 = 1.2$ ($\gamma = 180°$),	
		$V_2 = -1.9$ ($\gamma = 180°$),		$V_2 = 4.4$ ($\gamma = 180°$),		$V_2 = -2.2$ ($\gamma = 180°$),		$V_2 = 1.9$ ($\gamma = 0°$),	
		$V_3 = 1.4$ ($\gamma = 0°$)		$V_3 = 2.4$ ($\gamma = 180°$)		$V_3 = 0.6$ ($\gamma = 0°$)		$V_3 = 1.6$ ($\gamma = 0°$)	

The torsional potentials were defined as ($\Delta E^{QM} - \Delta E^{per}$), ΔE^{per} being defined in each case. ΔE^{QM} has been calculated at the HF/6-31 + *G*(*d*, *p*) and B3LYP/6-31 + *G*(*d*, *p*) levels.

V_n and γ (in kcal/mol and degrees, respectively) correspond to the potential barrier and the phase angle of a three-terms Fourier expansion (see Equation 2). The correlation coefficient r^2 is displayed in each case to indicate the goodness of the fitting.

changes associated to the variation of a dihedral angle. Therefore, the HF/6−31 + $G(d, p)$ should be considered as a suitable theoretical level for the parametrization of the torsional energy term.

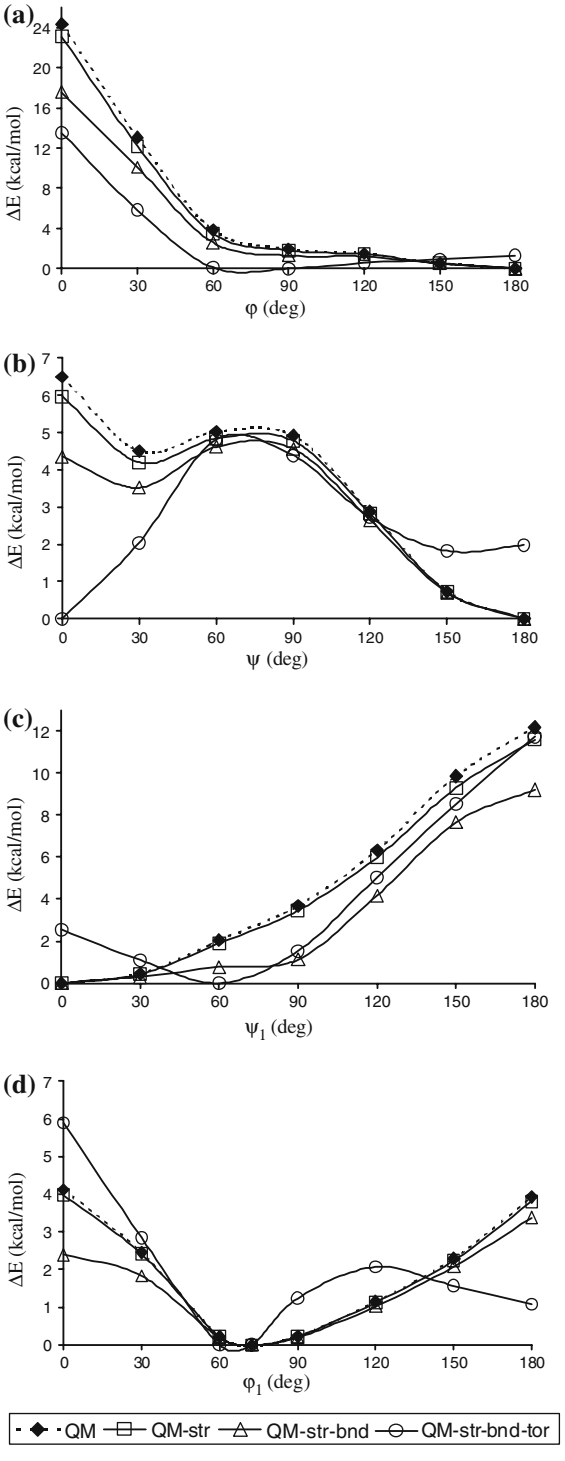

Influence of the bonding contribution in the torsional parameters

Table 1 lists the coefficients derived from the fitting of the ΔE^{QM} values to the Fourier expansion used to represent the dihedral interactions considering $\Delta E^{per} = 0$ (Equation 5), *i.e.* neglecting the variations in the molecular geometry different from the dihedral angle *j*. Although the statistical coefficient r^2 indicates an excellent fitting in all cases, the torsional parameters obtained using this approximation are contaminated by other energy contributions that are included in the rotational profile. This produces an overestimation of the barriers and, in some cases, a variation in the phase angles. In order to examine in detail the contribution of the bonding interactions to this term, we have considered the following three cases:

$$\Delta E^{per} = \Delta E_{stretching} \tag{7}$$

$$\Delta E^{per} = \Delta E_{stretching} + \Delta E_{bending} \tag{8}$$

$$\begin{aligned}\Delta E^{per} &= \Delta E_{stretching} + \Delta E_{bending} + \Delta E_{torsion}(i \neq j) \\ &= \Delta E_{bonding}\end{aligned} \tag{9}$$

Figure 3 shows the evolution of $(\Delta E^{QM} - \Delta E^{per})$ vs. the dihedral angle for such three cases, the variation of ΔE^{QM} being also displayed for comparison. Only the results derived at the HF/6−31 + $G(d, p)$ level are displayed, although those obtained using B3LYP/6−31 + $G(d, p)$ calculations provide very similar findings. As can be seen, the contribution produced by the stretching interactions is almost negligible in all cases, indicating that the bond lengths remain close to the equilibrium values during the whole profiles. Similarly, the contribution of the bending interactions to ΔE^{per} is small for **3** and **5**. However, a

Figure 3. Corrected energy profiles $(\Delta E^{QM} - \Delta E^{per})$ of the (a) N–C^{α} and (b) C^{α}–C rotations of **5**, (c) the C–C^{α} rotation of **1** and (d) the N–C^{α} rotation of **3**. The corrected profiles were calculated by removing from ΔE^{QM} the bonding energy contribution associated to the perturbation that the variation of the spanned dihedral angle causes in the other geometrical parameters of the molecule: $\Delta E^{QM} - \Delta E_{stretching}$ (QM–str), $\Delta E^{QM} - \Delta E_{stretching} - \Delta E_{bending}$ (QM–str–bnd), and $\Delta E^{QM} - \Delta E_{stretching} - \Delta E_{bending} - \Delta E_{torsion}(i \neq j)$ (QM–str–bnd–tor). The values of ΔE^{QM}, which are also displayed for comparison, were computed at the HF/6−31 + $G(d, p)$ level.

different behavior is observed for **1**, where the bending contribution cannot be neglected. Thus, a detailed analysis of the bond angles indicates that the ∠C–C$^{\alpha}$–C angle ranges from 121.3° to 112.0° through the whole rotational profile. This wide variation, which is produced by both strong repulsive interactions and electronic effects induced by the carbonyl groups, introduces a surplus of energy in the rotational profile that should not be included in the parametrization of the torsional interaction.

Finally, the contribution produced by the dihedral interactions is considerable, as reflects the reduction of the barriers and, in some cases, the change in the shape of the profiles. The latter is specially apparent in Figure 3b, where the conformation $\varphi, \psi = (180°, 0°)$ becomes a minimum after remove the contribution associated to the bonding interactions from the QM energy. The strong influence of the dihedral interactions is due to the following two factors: (*i*) the connection between the dihedral angles involved in the rotation of a given bond is not rigid, important deformations being allowed; (*ii*) the rotation around a given bond also affect the dihedrals of the bonds close in the space. Table 1 lists the torsional parameters derived from Equation 5 considering $\Delta E^{\text{per}} = \Delta E_{\text{bonding}}$ (Equation 9). As can be seen, the elimination of the bonding interactions produce a drastic changes in the torsional parameters of the three molecules.

Influence of the van der Waals and electrostatic contribution in the torsional parameters

Figure 4 shows the influence of van der Waals interactions in the QM rotational profiles. As can be seen, these short-range interactions are particularly relevant in **5** and **3** where the van der Waals contribution is higher than that produced by the sum of the bonding interactions. Interestingly, for **1** the influence of the van der Waals interactions is smaller than that provided by bonding interactions, even although in some calculated conformations the oxygen atoms of the two carbonyl groups are confronted. As was discussed above, the strength of the repulsive nonbonding interactions generated by such pair of atoms is partially

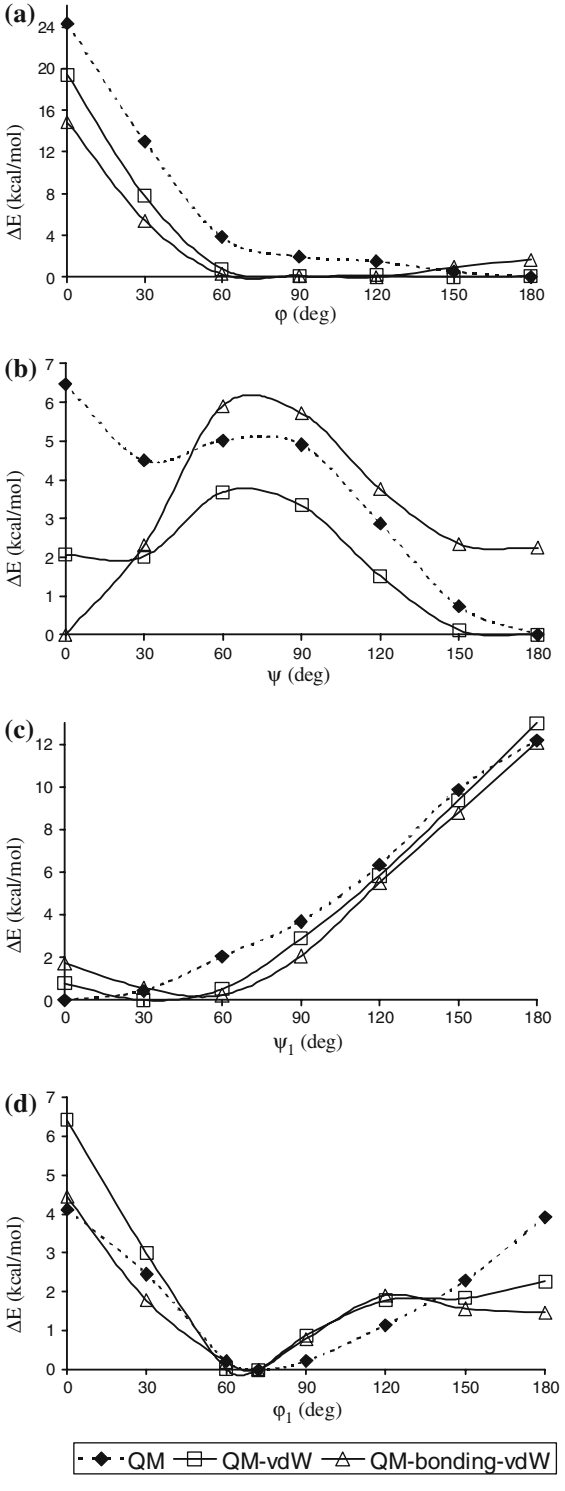

Figure 4. Corrected energy profiles $\Delta E^{\text{QM}}-\Delta E^{\text{per}}$ of the (a) N–C$^{\alpha}$ and (b) C$^{\alpha}$–C rotations of **5**, (c) the C–C$^{\alpha}$ rotation of **1** and (d) the N–C$^{\alpha}$ rotation of **3**. The corrected profiles were calculated by removing from ΔE^{QM} the van der Waals and bonding energy contribution associated to the perturbation that the variation of the spanned dihedral angle causes in the other geometrical parameters of the molecule: $\Delta E^{\text{QM}}-\Delta E_{\text{vdW}}$ (QM–vdW), and $\Delta E^{\text{QM}}-\Delta E_{\text{bonding}}-\Delta E_{\text{vdW}}$ (QM–bonding–vdW). The values of ΔE^{QM}, which are also displayed for comparison, were computed at the HF/6−31 + $G(d, p)$ level.

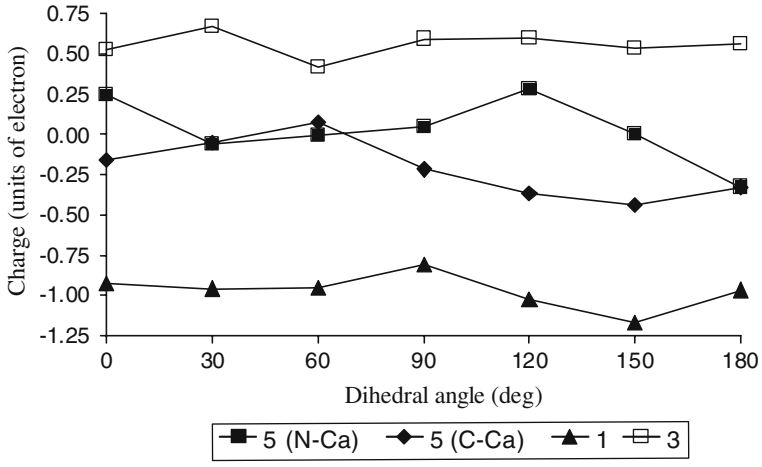

Figure 5. Evolution of the electrostatic charge on the C^{α} atom of **1**, **3** and **5** with the spanned dihedral angle.

mitigated by the distortion of some geometric parameters from their equilibrium values.

Two different approximations were used to estimate the contribution produced by the electrostatic interactions. The changes produced in the charge distribution upon alteration of the molecular conformation, *i.e*. geometry-dependent charge flux effects, have been considered in the first approximation, hereafter denoted A1. For this purpose, atomic charges have been recalculated for every conformation of each dipeptide. These geometry-dependent parameters should provide a satisfactory representation of the molecular electrostatic properties that depend on the molecular conformation. In the second approximation (A2), atomic charges were computed for the lowest energy conformation of each rotational profile, these electrostatic parameters being directly transferred to the rest of conformations. Thus, no dependence between the charges and the conformation was considered in this case, fixed charges being used for representing the relaxation of charge distribution that is dependent on changing the molecular structure dependent. Although different methods have been proposed to consider the geometry-dependent charge flux effects [47–50] the latter strategy is used more frequently in MM calculations.

Atomic charges change considerably with the conformation. This feature is illustrated in Figure 5, which shows the variation of the charge on the C^{α} atom of the glycine dipeptide and its retro-inverso modified analogues with the dihedral angle. Although the changes on **1** and **3** are very pronounced, the largest geometry-induced change occurs for **5**. Thus, the charge on the C^{α} atom of **5** decreases 0.5729 e.u. when the conformation change from φ, $\psi = (0°, 180°)$ to φ, $\psi = (180°, 180°)$. Figure 6 shows the $(\Delta E^{QM} - \Delta E^{per})$ profiles obtained for the investigated rotations considering

$$\Delta E^{per} = \Delta E_{bonding} + \Delta E_{vdW} + \Delta E_{electrostatic} \tag{10}$$

where $\Delta E_{electrostatic}$ corresponds to the torsional energy contribution produced by electrostatic interactions, which is evaluated using electrostatic parameters derived from approximations A1 and A2.

Interestingly, the values $(\Delta E^{QM} - \Delta E^{per})$ calculated using the A1 approximation are considerably larger than ΔE^{QM} values that may be interpreted as: electrostatic contribution induces a notable reduction of the torsional barrier. The origin of this physically unmeaning result is the dramatic overestimation of the electrostatic energy produced by geometry-dependent charges, as is illustrated in Figure 6. This amazing result can be attributed to a number of factors like, for instance, the limitation of the point charge model [51], the deficiencies of net atomic charges models to represent some molecules [52], the poor quality of MEP-derived charges on buried atoms [53], the neglection of distributed multiple moments [54], etc. Although the same factors are expected to appear in approximation A2, the consideration of

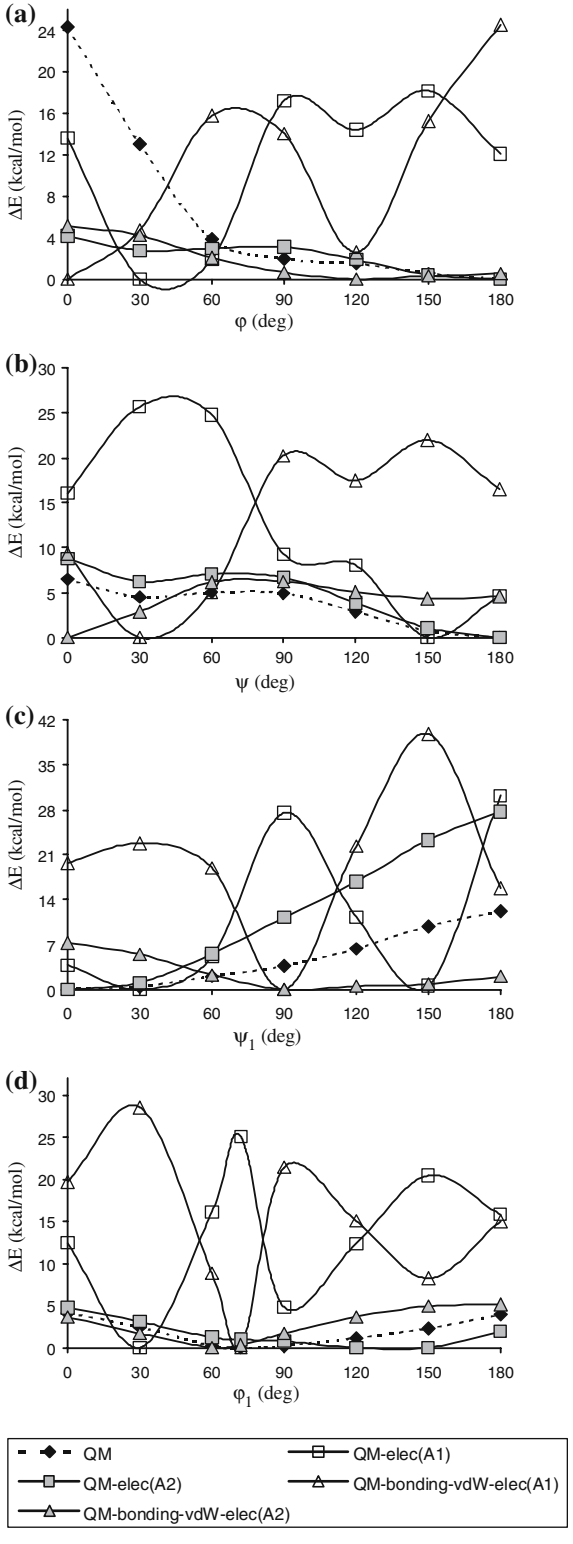

Figure 6. Corrected energy profiles $\Delta E^{QM}-\Delta E^{per}$ of the (a) N–C^{α} and (b) C^{α}–C rotations of **5**, (c) the C–C^{α} rotation of **1** and (d) the N–C^{α} rotation of **3**. The corrected profiles were calculated by removing from ΔE^{QM} the electrostatic, van der Waals and bonding energy contribution associated to the perturbation that the variation of the spanned dihedral angle causes in the other geometrical parameters of the molecule: $\Delta E^{QM}-\Delta E_{electrostatic}$ (QM–elec), and $\Delta E^{QM}-\Delta E_{bonding}-\Delta E_{vdW}-\Delta E_{electrostatic}$ (QM–bonding–vdW–elec). Electrostatic contribution has been computed according to approximations 1 and 2 (A1 and A2, respectively, see text). The values of ΔE^{QM}, which are also displayed for comparison, were computed at the HF/6–31 + $G(d, p)$ level.

fixed charges reduces the impact of these deficiencies by error cancellations.

Inspection to the variation of the electrostatic energy calculated using fixed atomic charges (A2 approximation) against the dihedral angle reveals a moderated contribution for all the molecules investigated. Consistently, the resulting ($\Delta E^{QM}-\Delta E^{per}$) values are smaller than ΔE^{QM}, which led to a reduction of the torsional energy when the contribution associated to these nonbonding interactions is removed. Table 1 lists the torsional parameters derived from Equation 5 considering $\Delta E^{per} = \Delta E_{bonding} - \Delta E_{nonbonding}$ (Equation 10) as calculated using the A2 approximation. As expected, these parameters are considerably smaller than those obtained using uncorrected ΔE^{QM} values. Furthermore, the energy barriers predicted for **5** agree satisfactorily with those predicted using the torsional parameters of standard force-fields.

Atomic charges proposed for the glycine residue and its retro-inverso modified analogues are displayed in Figure 7. As expected, charges predicted for the glycine residue are fully consistent with those reported in force-fields that used quantum mechanical MEPs for electrostatic parametrization [1, 7]. Retro-inverso modification produces significant changes in all the atoms, although these are more apparent in the C^{α}. The adjacent N–H withdrawal groups induce a positive charge in the C^{α} atom of **3**, the charges on the N atoms being more negative for the residue-contained in the latter molecule than that the N atom of the glycine residue. On the other hand, the electron donation of the adjacent C=O groups induces a very negative charge on the C^{α} atom of **1**.

On the other hand, it should be emphasized that parameters displayed in Table 1 have been obtained using the best fitting to a three-terms Fourier expression (Equation 2), the parameters provided

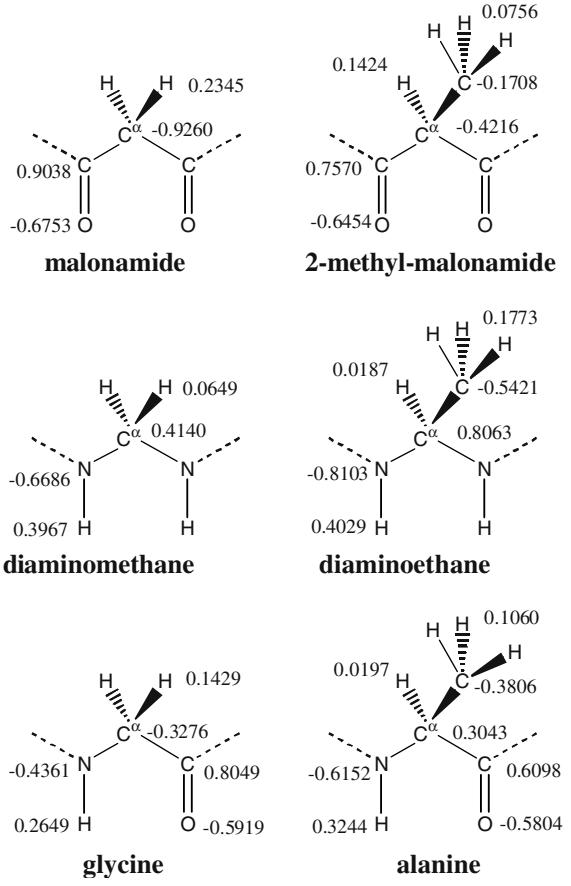

Figure 7. Atomic charges proposed for the glycine and alanine residues as well as their retro-inverso modified analogues. Charges have been derived from HF/6–31 + $G(d, p)$ calculations on the dipeptides displayed in Figure 1.

by such procedure being V_n and γ_n for $n = 1, 2$ and 3. Thus, other expressions that can be alternatively used to represent the torsional energy contribution have not been explored in this work. Accordingly, parameters listed in Table 1 are not comparable to those included in libraries of some standard force-field, where the potential energy function used to describe such energy term is different. However, the computational strategy employed in this work can be satisfactorily used in the development of torsional parameters independently of the analytical expression used to describe this energy term.

Parametrization of alanine and its retro-inverso modified analogues

Figure 8a and b shows the profiles $E = E(\varphi, \psi = 180°)$ and $E = E(\varphi = 180°, \psi)$, respectively, computed for alanine dipeptide, **6**, at the HF/6–31 + $G(d, p)$ level. These two rotational profiles remind those computed for **5**, the main differences being due not only to the stereochemistry at C^{α},

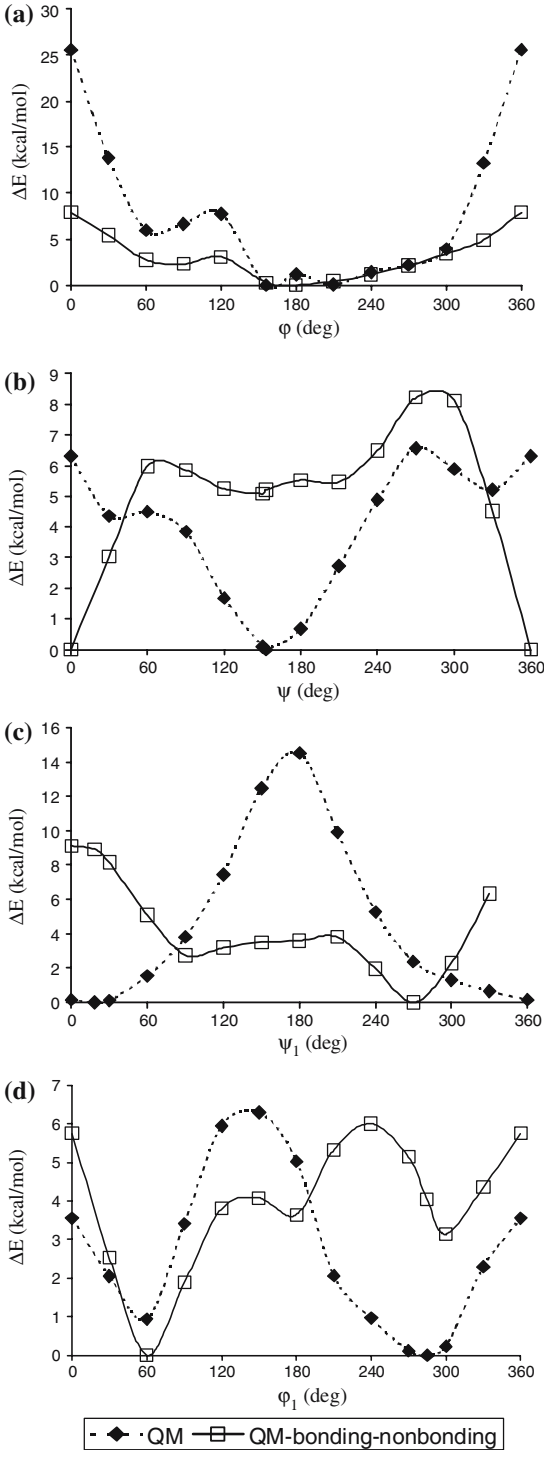

Figure 8. Quantum mechanical and corrected energy profiles $\Delta E^{QM}-\Delta E^{per}$ of the (a) N–C^{α} and (b) C^{α}–C rotations of **6**, (c) the C–C^{α} rotation of **2** and (d) the N–C^{α} rotation of **4**. The corrected profiles were calculated by removing from ΔE^{QM} the electrostatic, van der Waals and bonding energy contribution associated to the perturbation that the variation of the spanned dihedral angle causes in the other geometrical parameters of the molecule: $\Delta E^{QM}-\Delta E_{bonding}-\Delta E_{nonbonding}$ (QM–bonding–nonbonding). Electrostatic contribution has been computed according to approximations 2 (see text). The values of ΔE^{QM} were computed at the HF/6–31 + $G(d, p)$ level.

which breaks the symmetry at 180°, but also to the nonbonding interactions induced by the methyl group. Figure 8c and d display the profiles $E = E(\psi_1, \psi_2 = 180°)$ and $E = E(\varphi_1, \varphi_2 = 180°)$ calculated for **2** and **4**, respectively. The profile obtained for the former molecule is very similar to that calculated for **1** with a maximum clearly defined at $\psi_1, \psi_2 = (180°, 180°)$. On the other hand, comparison between **3** and **4** reveals that the methyl side chain induces a small change at the positions of the minima and the maxima, although the shape of the profiles is very similar for the two compounds.

The perturbation that the variation of a given dihedral angle causes in other geometric variables produces important changes in the bonding, van der Waals and electrostatic interactions. The importance of the contribution associated to such interactions in the torsional profiles of **6**, **2** and **4** was found to be similar to that showed above for glycine dipeptide and its retro-inverso modified analogues. Furthermore, electrostatic contribution was found to provide reliable results only when it is evaluated using fixed charges model, as was found for glycine dipeptide and its derivatives. Thus, geometry-dependent charges produce a notable increase of the torsional barrier after correct the energy profile by removing the electrostatic contribution, which is physically unreasonable.

Figure 8 compares the energy profiles ΔE^{QM} with $(\Delta E^{QM}-\Delta E^{per})$, where ΔE^{per} includes both bonding and nonbonding contribution (Equation 10), while Table 2 lists the resulting torsional parameters. Interestingly, the torsional parameters obtained for **6** are very similar to those displayed for **5** (Table 1). This concordance is fully consistent with that reported in the parameter libraries of the more employed force-fields [1–8], which use the same torsional parameters for glycine and alanine residues, supporting the goodness of our parametrization strategy. The opposite trend is detected when the results achieved for the retro-inverso modified peptides of glycine and alanine are compared. Thus, the torsional parameters predicted for **2** are different from those obtained for **1** and, similarly, the parameters of **3** differ from those **4**. This is probably due to the complex electronic distributions of retro-inverso modified dipeptides, which are altered by the methyl side chain of **2** and **4** with respect to those of **1** and **3**. This feature is illustrated in Figure 7, which shows the electrostatic charges of the different residues. Furthermore, Table 2 shows that the two fittings performed for **4** are very poor from a statistical point of view indicating that the three-term Fourier expansion employed in this work is not suitable to represent the

Table 2. Fitted parameters for the torsional potentials of alanine dipeptide and its retro-inverso modified analogues.

ΔE^{per}	**6** (N–C^{α})		**6** (C^{α}–C)		**2**		**4**	
	Parameters	r^2	Parameters	r^2	Parameters	r^2	Parameters	r^2
0		0.88		0.74		0.97		0.48
	$V_1 = 14.8$ ($\gamma = 0°$),		$V_1 = 4.8$ ($\gamma = 0°$),		$V_1 = 12.6$ ($\gamma = 180°$),		$V_1 = 2.2$ ($\gamma = 180°$),	
	$V_2 = -8.1$ ($\gamma = 180°$),		$V_2 = 2.2$ ($\gamma = 180°$),		$V_2 = -4.1$ ($\gamma = 180°$),		$V_2 = 2.2$ ($\gamma = 0°$),	
	$V_3 = 7.7$ ($\gamma = 0°$)		$V_3 = 0.7$ ($\gamma = 0°$)		$V_3 = 1.4$ ($\gamma = 180°$)		$V_3 = 1.1$ ($\gamma = 0°$)	
$\Delta E_{bonding}-$		0.94		0.82		0.89		0.52
$\Delta E_{nonbonding}$	$V_1 = 5.4$ ($\gamma = 0°$),		$V_1 = 2.7$ ($\gamma = 180°$),		$V_1 = 4.4$ ($\gamma = 0°$),		$V_1 = 3.4$ ($\gamma = 180°$),	
	$V_2 = -1.5$ ($\gamma = 180°$),		$V_2 = 4.6$ ($\gamma = 180°$),		$V_2 = 5.0$ ($\gamma = 0°$),		$V_2 = 3.2$ ($\gamma = 0°$)	
	$V_3 = 1.8$ ($\gamma = 0°$)		$V_3 = 3.1$ ($\gamma = 180°$)		$V_3 = -1.1$ ($\gamma = 180°$)		$V_3 = 0.1$ ($\gamma = 180°$)	

The torsional potentials were defined as $(\Delta E^{QM}-\Delta E^{per})$, ΔE^{per} being defined in each case. ΔE^{QM} has been calculated at the HF/6–31 + $G(d, p)$ level. V_n and γ (in kcal/mol and degrees, respectively) correspond to the potential barrier and the phase angle of a three-terms Fourier expansion (see Equation 2). The correlation coefficient r^2 is displayed in each case to indicate the goodness of the fitting.

dihedral interactions in this compound, *i.e.* more terms and/or different periodicities are necessary to improve the values of r^2.

Conclusions

In this paper we have used quantum mechanical calculations to develop torsional and electrostatic parameters for molecular mechanics studies of retro-inverso modified peptides. In order to obtain accurate torsional parameters, the whole energy profiles for the bond rotations were calculated scanning the appropriated dihedral angles and, subsequently, corrected by removing the energy contributions due to the modification of all the geometrical variables with exception of such dihedral angles. A detailed analysis of the results revealed that the perturbation exerted by the modification of the bonding, van der Waals and electrostatic interactions can produce drastic changes in both the shape of the profiles and the height of the barriers.

On the other hand, we examined different models to describe the electrostatic interactions. In all cases atomic charges were determined by fitting the rigorously computed quantum mechanical MEP to the classical one. Interestingly, the electrostatic model based on geometry-dependent charges led to erroneous results, which were physically unmeaning. Conversely, calculations with fixed charges produced results that are consistent with the chemical nature of retro-inverso modification. Accordingly, fixed electrostatic parameters have been proposed to perform MM simulations of peptides containing retro-inverso modified residues.

Finally, it should be mentioned that the parameters associated to the other terms of the force-field, *i.e.* stretching, bending and van der Waals, are expected to be transferable from conventional amino acids since they are not specially influenced by retro-inverso modification.

Acknowledgements

Authors are indebted to the "Centre de Supercomputació de Catalunya" (CESCA) and the "Centre Europeu de Paral lelisme de Barcelona" (CEPBA) for computational facilities.

References

1. Cornell, W.D., Cieplak, P., Bayly, C.I., Gould, I.R., Merz, K.M., , Jr., Ferguson, D.M., Spellmeyer, D.C., Fox, T., Caldwell, J.W. and Kollman, P.A., J. Am. Chem. Soc., 117 (1995) 5179.
2. Halgren, T.A., J. Comput. Chem., 17 (1996) 490.
3. Allinger, N.L., J. Comput. Chem., 17 (1996) 642.
4. Clark, M., Cramer, R.D., , III and van Opdenbosch, N., J. Comput. Chem., 10 (1989) 982.
5. Mohamadi, F., Richards, N.G.J., Guida, W.C., Liskamp, R., Lipton, M., Caufield, C., Chang, G., Hendrickson, T. and Still, W.C., J. Comput. Chem., 11 (1990) 440.
6. Chandrasekhar, I., Kastenholz, M., Lins, R.D., Oostenbrink, C., Schuler, L.D., Tieleman, D.P. and van Gunsteren, W.F., Eur. Biophys. J. Biophys. Lett., 32 (2003) 67.
7. MacKerell, A.D., Bashford, D., Bellott, M., Dunbrack, R.L., Evanseck, J.D., Field, M.J., Fischer, S., Gao, J., Guo, H., Ha, S., Joseph-McCarthy, D., Kuchnir, L., Kuczera, K., Lau, F.T.K., Mattos, C., Michnick, S., Ngo, T., Nguyen, D.T., Prodhom, B., Reiher, W.E., Roux, B., Schlenkrich, M., Smith, J.C., Stote, R., Straub, J., Watanabe, M., Wiorkiewicz-Kuczera, J., Yin, D. and Karplus, M., J. Phys. Chem. B, 102 (1998) 3586.
8. Kaminski, G.A., Friesner, R.A., Tirado-Rives, J. and Jorgensen, W.L., J. Phys. Chem. B, 105 (2001) 6474.
9. Rizzo, R.C. and Jorgensen, W.L., J. Am. Chem. Soc., 121 (1999) 4827.
10. Stewart, E.L., Nevins, N., Allinger, N.L. and Bowen, J.P., J. Org. Chem., 64 (1999) 5350.
11. Alemán, C., Proteins, 29 (1997) 575.
12. Balaram, P., Curr. Opin. Struct. Biol., 2 (1992) 845.
13. Chorev, M. and Goodman, M., Acc. Chem. Res., 26 (1993) 266.
14. Hintermann, T. and Seebach, D., Chimia, 51 (1997) 244.
15. Spatola, A.F., In Weinstein, B., (Ed.), Chemistry and Biochemistry of Amino Acids, Peptides and Proteins, Vol. 7. Marcel Dekker, New York, 1987, pp 267–357.
16. Chorev, M., Yaion, M., Wormser, U., Levian-Teitelbaum, D., Gilon, C. and Selinger, Z., Eur. J. Med. Chem., 21 (1986) 96.
17. Benedetti, E., DiBlasio, B., Pavone, V., Pedone, C., Fuller, W.D., Mierke, D.F. and Goodman, M., J. Am. Chem. Soc., 112 (1990) 8909.
18. Benedetti, E., Pedone, E.M., Kawahata, N.H. and Goodman, M., Biopolymers, 36 (1995) 659.
19. Fletcher, M.D. and Campbell, M.M., Chem. Rev., 98 (1998) 763.
20. Phan-Chan-Du, A., Petit, M.C., Guichard, G., Briand, J.P., Muller, S. and Cung, M.T., Biochemistry, 40 (2001) 5720.
21. Staubitz, P., Peschel, A., Nieuwenhuizen, W.F., Otto, M., Gotz, F., Jung, G. and Jack, R.W., J. Pept. Sci., 10 (2001) 552.
22. Bab, I. and Chorev, M., Biopolymers, 66 (2002) 33.
23. Fischer, P.M., Curr. Prot. Pept. Sci., 4 (2003) 339.
24. Volonterio, A., Bellosta, S., Bravin, F., Bellucci, M.C., Bruche, L., Colombo, G., Malpezzi, L., Mazzini, S., Meille, S.V., Meli, M., de Arellano, C.R. and Zanda, M., Eur. J. Chem., 9 (2003) 4510.
25. Lozano, J.M., Espejo, F., Ocampo, M., Salazar, L.M., Tovar, D., Barrera, N., Guzman, F. and Patarroyo, M.E., J. Struct. Biol., 148 (2004) 110.
26. Franco, L., Navarro, E., Subirana, J.A. and Puiggalí, J., Macromolecules, 27 (1994) 4284.

27. Alemán, C., Franco, L. and Puiggalí, J., Macromolecules, 27 (1994) 4298.
28. Aceituno, J.E., Tereshko, V., Lotz, B. and Subirana, J.A., Macromolecules, 29 (1996) 1886.
29. Alemán, C. and Pérez, J.J., J. Mol. Struct. (THEOCHEM), 285 (1993) 281.
30. Alemán, C. and Pérez, J.J., J. Mol. Struct. (THEOCHEM), 304 (1994) 17.
31. Alemán, C. and Puiggalí, J., J. Org. Chem., 60 (1995) 910.
32. Alemán, C., J. Biomol. Struct. Dyn., 14 (1996) 193.
33. Alemán, C., J. Phys. Chem. A, 105 (2001) 860.
34. Alemán, C. and Puiggalí, J., J. Polym. Sci. Part B. Polym. Phys., 34 (1996) 1327.
35. Alemán, C. and Bella, , J. Biopolym., 35 (1995) 257.
36. Stern, P.S., Chorev, M., Goodman, M. and Hagler, A.T., Biopolymers, 22 (1983) 1885.
37. Stern, P.S., Chorev, M., Goodman, M. and Hagler, A.T., Biopolymers, 22 (1983) 1901.
38. Dauber-Osguthorpe, P., Campbell, M.M. and Osguthorpe, D., J. Int. J. Pept. Protein Res., 38 (1991) 357.
39. Alemán, C., Canela, E.I., Franco, R. and Orozco, M., J. Comput. Chem., 12 (1991) 664.
40. Alemán, C. and Orozco, M., Biopolymers, 34 (1994) 941.
41. Alemán, C., Casanovas, J. and Galembeck, S.E., J. Comput. Aided Mol. Design, 12 (1998) 259.
42. Abrahao, O., Nascimento, P.D.B. and Galembeck, S.E., J. Comput. Chem., 22 (2001) 1817.
43. Alemán, C. and Muñoz-Guerra, S., J. Polym. Sci. Part B: Polym. Phys., 34 (1996) 963.
44. Namba, A.M., León, S., da Silva, G.V.J. and Alemán, C., J. Comput. Aided Mol. Design, 15 (2001) 235.
45. Cornell, W.D., Gould, I.R. and Kollman, P.A., J. Mol. Struct. (Theochem), 332 (1997) 101.
46. Gould, I.R., Cornell, W.D. and Kollman, P.A., J. Am. Chem. Soc., 116 (1994) 9250.
47. Winn, P.J., Ferenczy, G.G. and Reynolds, C.A., J. Phys. Chem. A, 101 (1997) 5437.
48. Mannfors, B.E., Mirkin, N.G., Palmo, K. and Krimm, S., J. Phys. Chem. A, 107 (2003) 1825.
49. Dinur, U. and Hagler, A.T., J. Comput. Chem., 16 (1995) 154.
50. Oda, A. and Hirono, S., J. Mol. Struct. (Theochem), 634 (2003) 159.
51. Surján, P. and Ángyan, J.G., Chem. Phys. Lett., 225 (1994) 258.
52. Williams, D.E., J. Comput. Chem., 15 (1994) 719.
53. Beck, B., Clark, T. and Glen, R.C., J. Comput. Chem., 18 (1997) 744.
54. Fowler, P.W., Chem. Phys. Lett., 176 (1991) 11.